Available online at www.sciencedirect.com
ScienceDirect
journal homepage: www.elsevier.com/locate/burns

The effects of pressure intervention on wound healing and scar formation in a Bama minipig model

Baimei Liu [a,b,c], Yang Liu [a,b,c], Li Wang [a,b,c], Chunsheng Hou [d], Meiwen An [a,b,c,*]

[a] Institute of Applied Mechanics and Biomedical Engineering, Taiyuan University of Technology, No. 79 Yingze Street, Taiyuan 030024, China
[b] Shanxi Key Laboratory of Material Strength & Structural Impact, College of Mechanics, Taiyuan University of Technology, No. 79 Yingze Street, Taiyuan 030024, China
[c] National Demonstration Center for Experimental Mechanics Education, Taiyuan University of Technology, No. 79 Yingze Street, Taiyuan 030024, China
[d] Department of Burns and Plastic Surgery, Taigang General Hospital, No. 213 North Street, Taiyuan 030009, China

ARTICLE INFO

Article history:
Accepted 5 September 2018

Keywords:
Scars
Pressure
IGF-1/IGF-1R
Signaling pathway

ABSTRACT

Pressure therapy has been widely used in clinical practice for the prevention or treatment of hypertrophic scars resulted from aberrations in wound healing. However, the precise molecular mechanisms of this process are only partially understood. In the present study, we established a Bama minipig model to observe the effect of pressure intervention on wound healing and scar formation. Transcriptome sequencing was performed to analyze the gene expression profiles in the injured and pressure-treated tissues. Furthermore, expression of the critical factors associated with IGF-1/IGF-1R pathways including PI3K/AKT and MEK/ERK and collagens were further analyzed by quantitative polymerase chain reaction (q-PCR) and Western blot. We observed that the mRNA expression of IGF-1 and IGF-1R were down-regulated in the pressure treated groups. Following pressure intervention, the trend in expression of PI3K/AKT decreased, whereas that of MEK/ERK expression increased, when quantified by q-PCR. Moreover, the level of PI3K protein expression decreased significantly after pressure treatment for one month but there was no significant difference in AKT protein expression. Interestingly, the trend in MEK/ERK protein expression was opposite to that indicated by q-PCR analysis. Furthermore, collagen I and III mRNA clearly declined after one month pressure treatment. Taken together, these results indicated that pressure intervention alleviated scar formation may via inhibiting the IGF-1/IGF-1R signaling pathway and collagen expression in the Bama minipig model.

1. Introduction

Hypertrophic scars (HSs) are pathological tissue structures resulting from aberrations in physiological wound healing after injury to the deep dermis resulting from burns, severe trauma or surgical procedures [1,2]. Excessive scarring is usually characterized by over-proliferation of fibroblasts, abnormal synthesis and degradation of extracellular matrix

* *Corresponding author at*: Institute of Applied Mechanics and Biomedical Engineering, Taiyuan University of Technology, No. 79 Yingze Street, Taiyuan 030024, China.
E-mail address: meiwen_an@163.com (M. An).
https://doi.org/10.1016/j.burns.2018.09.002

(ECM), disorders in regulatory cytokines and abnormal neovascularization [3–6]. Hypertrophic scars are generally raised, red, hard whilst in the form of a contracture, cause itching and painful. Patients with hypertrophic scars often experience serious cosmetic and functional problems and may experience both psychological and physiological effects [7,8]. It is therefore desirable to clarify the mechanism of formation of HSs and to seek effective and safe therapies to prevent their formation.

A variety of methods are used in the treatment of hypertrophic scars including surgical scar revision, corticosteroid injection, cryotherapy, radiotherapy and laser therapy. However, as some of the side effects of these modalities can be severe, their capacity to permanently eliminate HSs is limited [9–11]. Since the 1970s, hospitals around the world have used the pressure therapy to prevent and treat HSs [12–14]. Many studies have confirmed that pressure therapy could reduce excessive scarring among burn patients [15–17]. In a recent evidence-based practice review by Sharp et al., pressure therapy was recommended as a successful scar treatment due to the resulting improvement in esthetic outcomes reflecting in the decreased erythema and height of scars [18]. According to the clinical studies, pressure therapy is deemed to induce hypoxia, ischemia and deficiency of nutrition and reduce collagen deposition within a developing or active scar [19–21]. Additionally, pressure garments often mitigate the pain or itch related to hypertrophic scars and tend to prevent the progression of severe contractures [22,23]. However, the outcome of pressure therapy has only ever been evaluated through clinical experience, a detailed analysis of the molecular mechanisms involved was rarely scientifically described [24]. An exploration of the therapeutic and preventive techniques using pressure has thus become an important research direction in the area of hypertrophic scarring.

Although many experiments in laboratory and clinical studies have been performed, the mechanisms of scar formation are still unclear, mainly because the phenomenon is observed solely in humans and the consecutive acquirement of tissue samples from humans is difficult. Animal models could help to illuminate the mechanisms of scar formation and promote the investigation and development of new therapies.

Hypertrophic scarring in an ideal animal model should match humans in their appearance, histological aspects, clinical behavior, biochemistry, molecular biology. Morris et al. reported that they established a hypertrophic scar model through creating excisional wounds over the surface of rabbit ear. In their animal model, the wounds were small and full-thickness, unlike the burn wounds which were large and partial-thickness. And the deep dermis was uninjured after burn injury [25]. The skin of the Bama minipig is very similar to that of human skin, comprising collagen, elastic and mesh fibers, with no significant difference in thickness of the cuticle layer, epidermis or dermis in the pig compared to an adult human [26,27]. In addition, the reaction of the pig to trauma is similar to humans where wounds repair principally by epithelialization, whereas in rodents, the wound first shrinks in order to begin the repair of traumatic injuries [28]. The similarities with porcine physiology suggest that the pig, particularly the miniature pig, could be used as a model for wound repair. The Bama minipig (*Sus scrofa*), a breed of naturally-occurring minipig in China, is a hopeful basis for creating an animal model.

The insulin-like growth factor (IGF)-1/IGF-1 receptor (IGF-1R) axis is proved to play a crucial role in the scar formation, by inducing collagen synthesis and secretion of extracellular matrix by fibroblasts and inhibiting apoptosis, thus influencing tissue reconstruction following wound healing [29,30]. Previous studies suggested that IGF-1 and its receptor are the principal regulators of anti-apoptotic signals [31]. In a model of apoptosis induced in culture *in vitro*, physiological concentrations of IGF-1 can effectively prevent c-myc fibroblast apoptosis, and maintain their survival [32]. Researchers have detected abundant expression of IGF-1 receptors in fibroblasts within hypertrophic scars and keloids, which may inhibit apoptosis or change the balance of cell proliferation and apoptosis, causing large quantities of extracellular matrix to be expressed and deposited [33]. The MEK/ERK and PI3K/AKT pathways were reported as downstreams of IGF-1/IGF-1R, which were implicated in scar formation [34,35].

In the current study, we investigated the effect of pressure on the process of wound healing and scar formation in a Bama minipig model, and also explored the possible molecular mechanisms. Our results indicated that pressure exerted an important role in wound healing and its application alleviated scar formation. The finding demonstrated that pressure intervention can ameliorate the excessive deposition of scar tissue and improve the appearance of the healed wounds.

2. Materials and methods

2.1. Animals

Adolescent female Bama miniature pigs (n = 4) aged 2–3 months and weighing 21–23 kg were used for this study. They were purchased from the Beijing Shichuang Century Minipig Breeding Base and raised in the Center for Drug Safety Evaluation, China Institute For Radiation Protection and cared for by an experienced technician. The animals were raised in single cages indoors and given lab porcine grower diet and water three times per day. They were acclimatized for 2 weeks before initiation of the experiment. The animal experiments and surgery were carried out according to the Animal Care and Use Committee of the Shanxi Science and Technology Department.

2.2. Skin wounding

Each animal was fasted for 12 h before surgery. The hair on its back was shaved and the betadine solution and 75% alcohol were used to disinfect dorsal skin thoroughly. The animals were pre-medicated with Zoletil (15 mg/kg) by intramuscular injection 10 min before skin wounding commenced. When complete anesthesia had been achieved, the pigs were placed in ventral recumbency on the operating table. Four deep dermal wounds, 8 × 8 cm were created on the back of each pig in two rows of two columns. The deep dermal wounds, which were demonstrated to produce HSs [36], were produced with an electric dermatome for 1.8 mm in depth (Tyler Research Corp., Edmonton, AB). Nevertheless, the actual wound depth is variable due to the diversiform, uncontrollable reasons when obtaining the wounds with a dermatome. The wounds were denoted left front, left rear, right front or right rear, depending on their position. Bandages were applied after wound hemostasis was achieved, and then removed after 24h and the wounds allowed to heal in the open without application of topical agents or dressings.

2.3. *Pressure treatment*

Sixty days after surgery, the healing progress and scar condition of all the minipigs samples were the same. Therefore, a homemade elastic knitted device designed to exert a pressure of approximately 3.4kPa (25.5mmHg) on the underlying tissue was applied to the two front wounds and the two rear wounds were as control group. This professional and commercial elastic fabric contains 41% spandex fiber and is plain-knitted structure. It can provide 20–40mmHg medical standard pressure and its elastic recovery ratio is more than 80%. The material is provided by the department of burns and plastic surgery, Taigang General Hospital, where it is used to make pressure suits for scar patients. A sensor (LKH-127) made of alloy steel and purchased from Nanjing Lanke Automation Equipment Co., Ltd (China) was used to measure the pressure once a week to ensure the size was adjusted appropriately. It is designed to exert 0–5kPa pressure by the company according to our measurement requirements in the experiment. The pressure measurement and adjustment results in detail was shown in Table 1.

2.4. *Tissue sampling*

A digital camera was used to evaluate macroscopic changes within the wound bed, making comparisons with normal skin removed at the beginning of the surgery. At day 0 (normal skin), 14, 30, 60, 90 and 120 post-injury, the animals were anesthetized, and tissue samples were collected from each dorsal wound down to the subcutaneous fascia using a surgical blade, for histological and molecular analysis. Each sample was divided into three pieces for either histology or molecular analysis, in which case they were placed in liquid nitrogen to be frozen immediately then stored at −80°C until processed. Because the pressure applying was initialed at 60day post injury, therefore, the samples treated with pressure for 30days (1 month) at 90day post injury was defined as '90d+P' and the controlled group was defined as '90d'; the samples treated with pressure for 60days (2 month) at 120day post injury was defined as '120d+P' and the controlled group was defined as '120d'.

2.5. *Histological examination*

Samples from normal skin and scar tissue with and without pressure treatment were placed into 4% paraformaldehyde immediately after harvesting from the pigs, then embedded in paraffin blocks. 5 μm-thick sections were prepared for subsequent tissue processing. Masson's trichrome and hematoxylin and eosin (H&E) staining were performed to analyze collagen fibers, then photographed using optical microscopy. All samples were evaluated in a blinded manner.

2.6. *mRNA sequencing*

Gene expression was investigated at the transcriptional level using high-throughput Illumina sequencing technology and bioinformatics tools. Total RNA was extracted from HS samples using a *mir*Vana™ miRNA isolation kit (Cat#AM1561, Ambion) according to the manufacturer's instructions. The RNA quantity was measured using a NanoDrop Spectrometer (ND-1000 Spectrophotometer, Peqlab). The RNA integrity number (RIN) was tested using an Agilent Bioanalyzer 2100 (Agilent Technologies, Santa Clara, CA, USA). And qualified total RNA was further purified using an RNAClean XP Kit (Cat A63987, Beckman Coulter, Brea, CA, USA) and RNase-free DNase set (Cat#79254, Qiagen GmbH, Germany). The RNA of each tissue sample that passed quality control testing was used for constructing the library. Poly-T oligo-attached magnetic beads were used for purifying the Poly-A containing mRNA molecules. After purification, the mRNA was fragmented into small pieces using divalent cations at 94°C for 8min. The cleaved RNA fragments were copied into first-strand cDNA using SuperScript II Reverse Transcriptase (Invitrogen, 18064014, Carlsbad, CA, USA) and random primers, followed by second-strand cDNA synthesis using Second Strand Master Mix and isolation using AMPure XP beads (A63881, Beckman). The cDNA fragments then underwent an end repair procedure, a single 'A' base was added and they were then ligated to adapters. The products were purified and then enriched using PCR to create the final cDNA library. Purified libraries were quantified using a Qubit® 2.0 Fluorometer (Life Technologies, USA) and validated using an Agilent 2100 bioanalyzer (Agilent Technologies, USA) to confirm insert size and calculate its molar concentration. Clusters were generated using a cBot with the library diluted to 10pM and sequenced on an Illumina HiSeq 2500 (Illumina, USA). Library construction and sequencing were performed by Shanghai Biotechnology Corporation (Shanghai, China).

2.7. *Data analysis for gene expression*

The sequenced raw reads were preprocessed via filtering out those from rRNA, short-fragment reads, low-quality reads and other sequence adapters, yielding a dataset consisting of clean tags. The cleaned reads were mapped to a pig (*Sus scrofa*) reference genome with two mismatches using Tophat v2.1.0. The number of fragments per kilobase of exon per million mapped reads (FPKM) was used to calculate gene expression.

Table 1 – Weekly pressure measurement and adjustment results using pressure sensors.

	Week 0	Week 1	Week 2	Week 3	Week 4	Week 5	Week 6	Week 7	Week 8
Pressure measured (kPa)	3.4	3.3	3.2	3.2	3.2	3.3	3.2	3.2	3.2
Pressure adjusted (kPa)	–	3.4	3.4	3.4	3.4	3.4	3.4	3.4	3.4

Cuffdiff software was used to identify differentially expressed genes (DEG). In multiple tests, the significance threshold of the p-value is determined by the false discovery rate (FDR).

2.8. Validation with qRT-PCR

The genes associated with the IGF-1/IGF-1R signaling pathway were selected to validate the veracity of RNA-seq by quantitative real time PCR (qRT-PCR) using the same RNA samples as in the RNA-seq. Total RNA was extracted and purity calculated from the optical density (OD) ratio (260 nm/280 nm). The ReverTra Ace qPCR RT Kit (Toyobo, Japan) was used to performe cDNA synthesis abiding by the manufacturer's instructions. All samples were reverse transcribed simultaneously to avoid experimental variation. The qPCR experiments were performed using Power SYBR® Green PCR Master Mix (ABI, USA), templates and primers in a total reaction volume of 10 μL. A 7900 HT Sequence Detection System (ABI, USA) was used with the following cycling parameters: denaturation at 95 °C for 10 min, followed by 40 cycles of 15 s at 95 °C then 1 min at 60 °C. The relative expression of the target genes were normalized against the expression level of succinate dehydrogenase (SDHA) using the $2^{-D\Delta Ct}$ method. All mRNA primers were designed and synthesized by Sangon Biotech (Shanghai, Co., Ltd.). The primer sequences (*Sus scrofa*) used for gene amplification were shown in Table 2.

2.9. Western blotting

After treatment with pressure, specimens were harvested and homogenized in 200 μL lysis buffer (C510003-0050, Sangon Biotech, Shanghai, China). The lysates were centrifuged at 4 °C, 13,000 rpm, for 10 min, and then the supernatants were harvested. The concentration of protein in each tissue sample was measured using a bicinchoninic acid (BCA) protein assay kit (C503021-0500, Sangon Biotech, Shanghai, China) following the manufacturer's protocol. A proper volume of loading buffer was added to each sample followed by thermal denaturation, 100 °C for 5 min. 20 μg total protein were separated using SDS-PAGE and then transferred onto a polyvinylidenedifluoride (PVDF) membrane at low temperature. After blocking with 5% skimmed milk and washing, the membranes were probed/incubated with primary antibodies to PI3K (1:1000), AKT2 (1:500), MEK1/2 (1:500), and ERK1/2 (1:1000) at 4 °C overnight. The membranes were subsequently incubated with a secondary antibody, which was connected with a fluorescence dye. In order to ensure equal loading, beta-actin (Abcam, Cambridge, MA, USA) was used as an internal standard. Enhanced chemiluminescence detection (ECL) reagents and a gel imaging system (Tanon Science & Technology Co., Ltd., China) were used to visualize protein bands. A densitometer (imaging system) was used to determine the protein expression. Experiments were performed in triplicate. The relative levels of protein expression were compared with that of the normal skin (defined as 1.00).

2.10. Statistical analysis

Data were processed using SPSS 16.0 software, presented as mean ± standard deviation. Differences were compared among the groups with one-way ANOVA. Significant difference with respect to control groups, P value <0.05.

Table 2 – Forward and reverse primer sequences of genes associated with the IGF-1/IGF-1R signaling pathway and collagen.

Gene name	Gene description	Genebank No.	Primer sequence (5′ to 3′)
IGF-1	Insulin-like growth factor 1	397491	F TCCTGAAGAGTGAAGAATGACA R GGAATGCCCATCTTTTGAA
IGF-1R	Insulin-like growth factor 1 receptor	397350	F TCATCAGCAGCATCAAGGAC R CGGCTTGTTCTCCTCACTGT
PI3K	Phosphatidylinositol-3-kinase	100514626	F TGGGATTCAAGCATTGTGGC R TGGGGCTTCATTCCTTTTTGA
AKT2	AKT serine/threonine kinase 2	100127478	F GAGGTCATGGAGCACAGGTT R CGTCAAAGTACCGAGTGTCG
MEK1	Mitogen-activated protein (MAP)/extracellular signal-regulated kinase (ERK) kinase 1	100233191	F GCTTGGGGCTATTTTTGTGT R ACGGTGTGGGAGAGCAGT
MEK2	Mitogen-activated protein (MAP)/extracellular signal-regulated kinase (ERK) kinase 2	100525505	F GAGAGCCTCACAGCATCTCG R TAGGAGGTGGCTCGTTCACA
ERK1	Extracellular signal-regulated kinase 1	445013	F TCCTTACCTGGAGCAGTACTACGA R AGCTCCATGTCGAAGGTGAAA
ERK2	Extracellular signal-regulated kinase 2	100153927	F CACAACACCTCAGCAATGACC R AGCAGGTTGGAAGGCTTGAG
COL1A2	Collagen type I alpha 2 chain	100626716	F AACCATGAACATTTGCACCA R GGTATGGATCACACTCACAGGA
COL3A1	Collagen type III alpha 1 chain	100152001	F TTGGCATTCCTTCGACTTCT R TGTTCCATGTACGCAATGCT
SDHA	Succinate dehydrogenase complex flavoprotein subunit A	780433	F CACACGTTGTACGGAAGGTCT R ATCAGGAGATCCAAGGCAAA

3. Results

3.1. *The effect of pressure intervention on macroscopic appearance*

Gross changes in the general appearance and size of the wounds were observed at different time points. Representative examples of pressure-treated and untreated wounds and scars at different time points are shown in Fig. 1. On the 14th day after injury, granulation tissues were observed to fill with in all wounds, and partial re-epithelialization appeared at the edge of the wound. From day 30 until the end of the experiment, all wounds were observed to present a dense, fibrotic and raised appearance compared to the surrounding uninjured skin, but the raised scars were not as much as human hypertrophic scars and the skin scars of previously reported female red Duroc pigs [37]. The scar at 60days was within the original margin range, clearly tougher than the surrounding normal skin, appearing deep red in the center. Furthermore, in comparison to the untreated group, the pressure-treated group exhibited a pigmented area that was smaller, with less contraction and some softening of the scar surface, and the size of wounds was smaller. This might due to the decrease of blood vessel in the scar tissue, leading to a low supplication of oxygen and nutrient for cellular activity.

3.2. *The effect of pressure intervention on histological level*

HE and Masson staining were performed to detect the effect of pressure intervention on histological wound morphology (Fig. 2). There were few fibroblasts in normal skin, and the vascular cavity was smooth and evenly distributed. Collagen fibers were parallel to the surface and had a loose and orderly arrangement. A large number of hair follicles and other skin attachments can be seen. However, the dermis in the wounds and scars was clearly thickened. By day 30, the wounds contained an organized dermis, epidermis also being partly present. Numerous fibroblasts were present with a disordered arrangement of collagen bundles, visible changes in coiling and nodular distribution were observed. After 60 days, the boundary was not clear between the dermal papilla and reticular layers. Granulation tissue was present in all samples. The resulting scars were histopathologically identical to human hypertrophic scars [38]. However, the connective tissues were thinner after one month pressure intervention. Besides, the collagen bundles were regular and parallel to the surface as observing in normal skin after two months pressure intervention.

3.3. *The effect of pressure intervention on the transcriptome level*

RNA sequencing was performed to further understand the potential mechanisms of pressure intervention. We selected 11 genes associated with wound healing and scar formation to analyze mRNA expression (Tables 3 and 4). Then the RNA-seq results of the above genes were verified by qRT-PCR. As shown in Fig. 3, applying pressure for one month significantly decreased IGF-1 mRNA levels compared with untreated group ($p<0.01$). By contrast, applying one-month pressure to the scars did not present dramatic effects on the IGF-1R, whereas the expression decreased to a level similar to that of normal skin after two months pressure treatment. Interestingly, similar results were observed in the expression profile of PI3K and AKT2 after two months pressure treatment. Moreover, MEK1/2 and ERK1/2 mRNA expression were increased after pressure intervention, whereas collagen I and II mRNA expression were strongly suppressed after one month pressure treatment. The qRT-PCR results showed an accordant trend to RNA-seq, indicating that the transcriptome sequencing results were reliable and accurate.

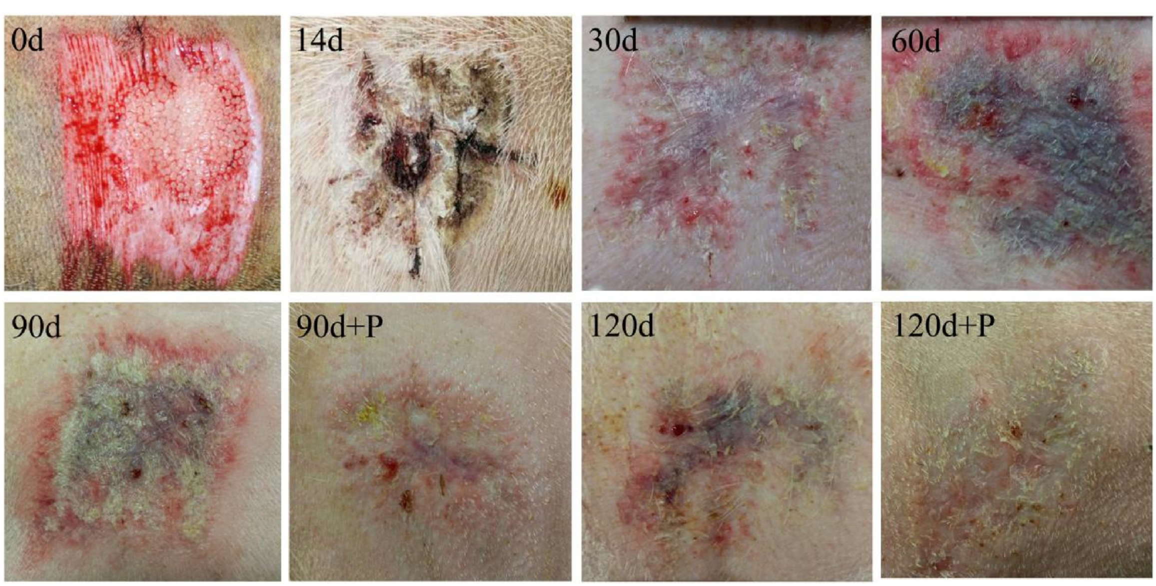

Fig. 1 – Representative macroscopic overview of wounds and scars on the back of Bama minipig at various time points. Pressure of 3.4kPa was applied at 60days post-injury for one month (90d+P) and two months (120d+P), the untreated wounds (90d) and (120d) were as controlled. Pressure intervention improved wound healing and alleviated scar formation.

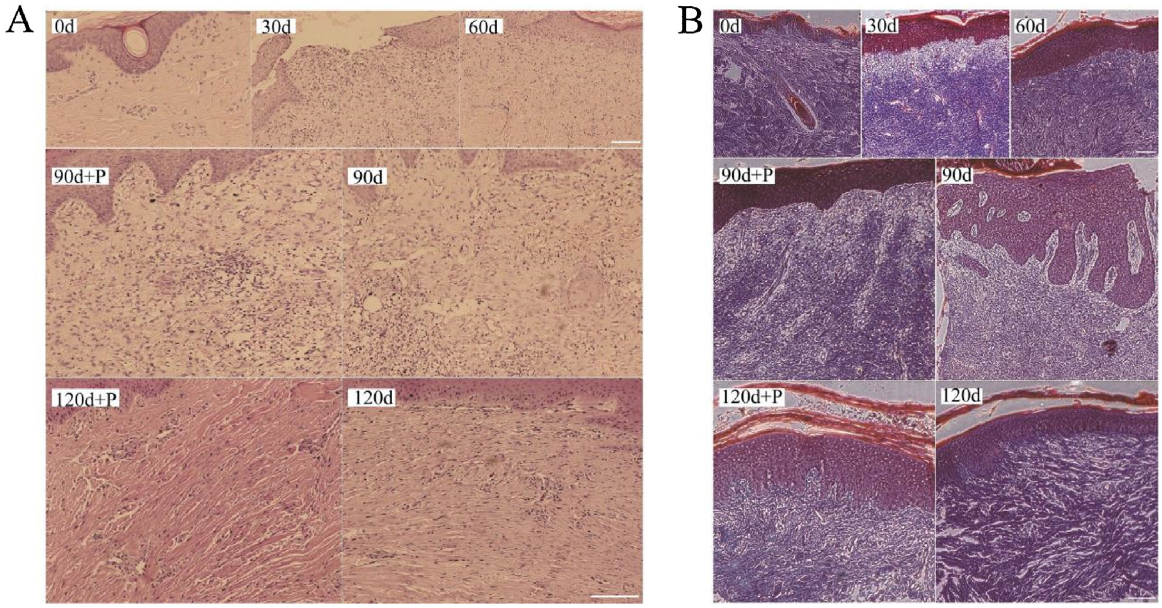

Fig. 2 – Representative histological images of wounds and scars at various time points. (A) HE staining images of wounds and scars treated with or without pressure at various time points. (B) Masson's trichrome-stained images of wounds and scars treated with or without pressure at various time points. (Original magnification × 100; bar = 100 μm).

Table 3 – Change in gene expression in wounds and scars: ratio of values for wounds and scars/normal skin.

Gene name	Ratio of gene expression of wounds and scars/normal skin						
	14d	30d	60d	90d+P	90d	120d+P	120d
IGF-1	1.02	7.11	9.03	2.18	3.87	8.37	2.01
IGF-1R	0.70	0.68	0.72	0.62	0.73	0.91	1.10
PI3K	0.44	1.20	1.36	0.94	1.00	1.55	1.30
AKT2	1.17	0.90	0.76	1.02	0.82	0.78	0.85
MEK1	1.38	2.76	1.74	1.39	1.86	1.13	0.52
MEK2	1.32	0.68	0.74	0.99	0.65	0.81	0.70
ERK1	1.52	1.30	1.35	1.18	1.08	1.55	1.10
ERK2	1.08	1.01	0.80	1.39	1.11	0.93	0.67
COL1A2	10.06	122.23	62.95	4.12	109.02	7.32	1.37
COL3A1	10.30	142.24	82.26	5.36	121.66	7.50	1.34

Table 4 – Change in gene expression in scars: ratio of values for pressure/no pressure.

Gene name	Ratio of expression for pressure/no pressure	
	90 d	120 d
IGF-1	0.56	4.16
IGF-1R	0.85	0.83
PI3K	0.94	1.19
AKT2	1.24	0.92
MEK1	0.75	2.17
MEK2	1.52	1.16
ERK1	1.09	1.41
ERK2	1.26	1.39
COL1A2	0.04	5.34
COL3A1	0.04	5.60

3.4. *The effect of pressure intervention on the protein expression*

The protein levels of relevant genes in wounds and scars treated with or without pressure were quantified using Western blot. An obvious downstream candidate of IGF-1/IGF-1R signaling is the PI3K/AKT pathway, which is thought to be induced mechanically. In our model, the PI3K protein level decreased in mechanically-stressed wounds compared with control wounds at 90 days but increased at 120 days post injury ($P < 0.05$) (Fig. 4). Wound homogenates showed no significant changes in the expression of activated AKT2/AKT3 protein in the mechanically-loaded wounds compared with controls at 90 and 120 days post injury. Since the MEK/ERK pathway also fulfills a crucial role in scar formation and development, we next investigated whether application of pressure affected the

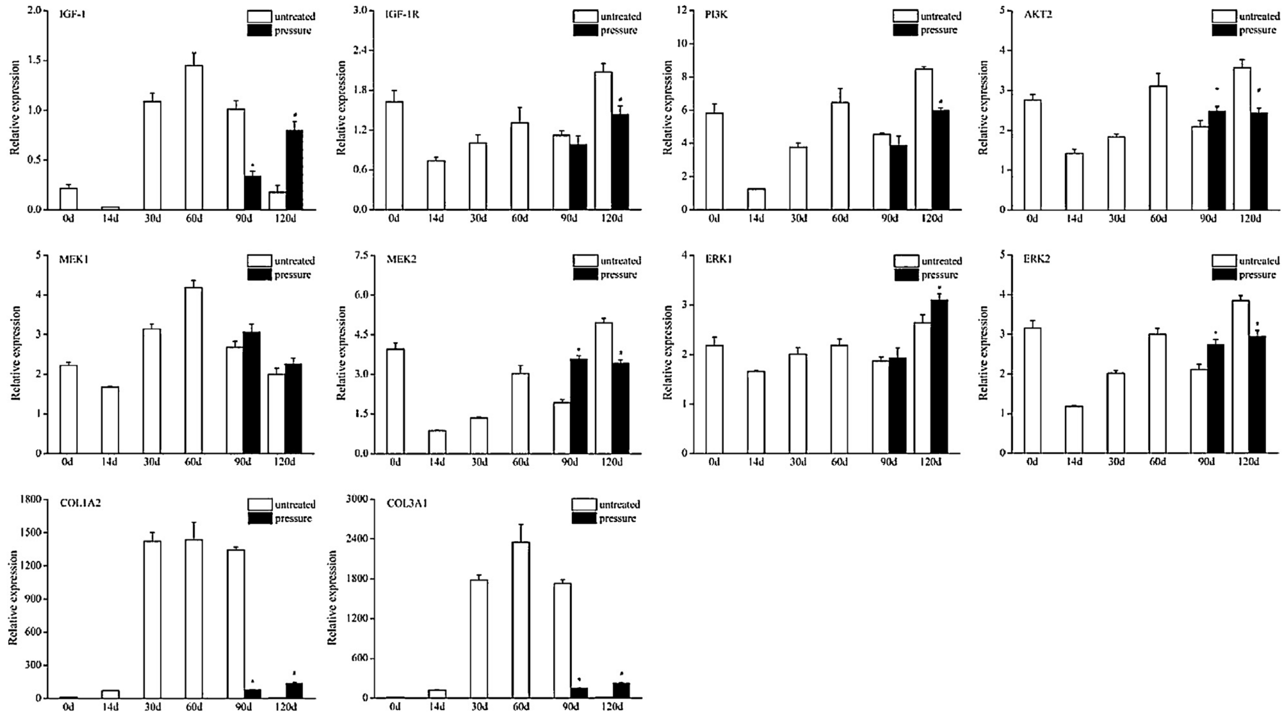

Fig. 3 – Genes related to the IGF-1/IGF-1R signaling pathway and collagen mRNAs were determined by qRT-PCR. The white bars represent wounds and scars without pressure treatment, the black bars represent scars with pressure treatment. The results are mean ± SD of three independent experiments. (*P < 0.05 compared with the untreated samples at 90 days; #P < 0.05 compared with the untreated samples at 120 days).

level of MEK/ERK protein expression. The results demonstrated that pressure treatment significantly inhibited the expression of MEK/ERK after one and two months pressure application.

4. Discussion

In this study, a Bama minipig model was established to observe the effect of pressure intervention on wound healing and scar formation. We evaluated the gross and clinical appearance, histological and molecular changes to validate the reliability of the model. The results showed sufficient similarities to those observed in the red Duroc pig model and human scars. Currently, pressure therapy is widely used in the prophylaxis and treatment of hypertrophic scars because of its effectiveness and convenience, but there is no clear understanding of its specific mechanism [39,40]. Furthermore, the 15 mmHg pressure was proved to be effective but not greater than 40 mmHg [41]. Besides, it is believed that the clearest effect of pressure treatment is when burn scars are still in their hyperactive phase less than 6 months. This animal model, in which 3.4 kPa pressure was applied for two months after trauma, met the conditions of early intervention and treatment for scars in clinic. Meanwhile, it also provided the possibility of continuous extraction of specimens, which is not practicable or ethical in clinical research of scars in humans.

Previous studies have provided evidence that the abnormal activity of growth factors and receptors play a vital role in the development of pathological scars [3,42,43]. Furthermore, the IGF-1/IGF-1R pathway has been demonstrated to be involved in plenty of fibrotic diseases, including scars and keloids [44]. It is well established that IGF-1 is a mitotic and differentiated factor that promotes wound healing by stimulating fibroblast proliferation, inhibiting apoptosis and improving collagen synthesis [45–47]. Thus, we investigated the roles of the IGF-1/IGF-1R pathway in response to pressure in this study. Our results showed that increased mRNA expression of IGF-1 in scar tissues collected from 30 and 60 days post injury was consistent with a previous study conducted by Gallant-Behm [48]. Not only IGF-1, but IGF-1R was also down-regulated in the pressure-treated group compared with untreated group, in spite of higher than that of normal skin. The reduced secretion of IGF-1/IGF-1R may slow the proliferation of scar fibroblasts and therefore inhibit the production of collagen fibers, explaining why pressure alleviated scar formation presented here.

According to the classical model, MAPK and PI3K pathways are the two major downstream signaling pathways which play crucial roles in inducing cell proliferation and inhibiting cell apoptosis by IGF-1R. Activation of PI3K pathway induced phosphorylation of Ser473 and Thr308 residues on AKT, thus activating this kinase [25]. Furthermore, it is reported that AKT acts as a pro-survival marker promoting cell survival. Our results showed that when scars were treated with pressure for two months, the expression of PI3K and AKT were down-regulated compared with no-pressure conditions. This suggests that mechanical pressure may inactivate the PI3K/AKT pathways, leading to a decreased accumulation of cells in scars. We have also shown here that in the process of scar

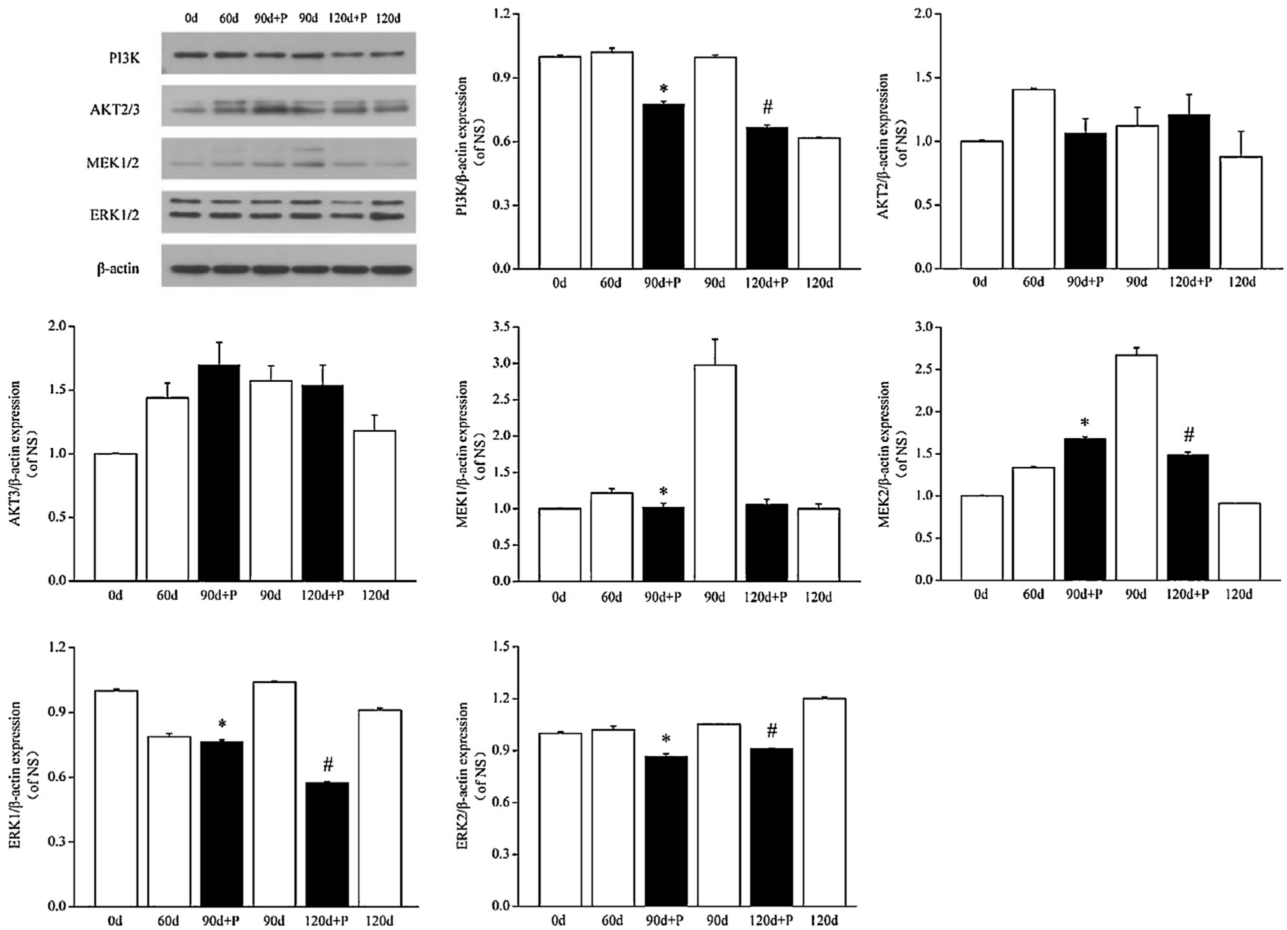

Fig. 4 – Western blot analysis of proteins related to the IGF-1/IGF-1R signaling pathway in the Bama minipig model. Histograms relate to a quantitative analysis of protein levels using Image-Pro Plus. The results are mean ± SD of three independent experiments. (*P < 0.05 compared with the untreated samples at 90 days; #P < 0.05 compared with the untreated samples at 120 days).

formation, the expression of MEK changed from a low level at 14 days to a high level at 60 days. In addition, the ERK signaling pathway was activated in response to pressure. It has previously been demonstrated that scarring in the rabbit ear model is related to ERK and JNK-mediated collagen I expression [49]. As the MEK/ERK signaling pathways play crucial roles in regulating the different biological activities of scar fibroblasts including cell migration and apoptosis, the role of the MEK/ERK signaling pathway observed here requires further investigation. In brief, our results suggest that a better understanding of the MAPK and PI3K signaling pathway in pressure therapy may provide novel targets to treat scars. The common view is that scar formation is the result of excessive deposition and reduced degradation of ECM [4]. After skin injury, growth factors stimulate a mass of fibroblast proliferation and excessive synthesis of ECM, particularly collagen I and collagen II [50,51]. In our study, pressure intervention suppressed the expression of collagen, causing the level decrease to that in normal skin.

Clinically, the pressure garment for burn patients to treat scars can be made of different materials such as nylon. The properties and pressure size of the garment are often affected by the type of fiber and the method of fabric construction [52,53]. In the current study, a homemade elastic knitted device contained 41% spandex fiber was applied to perform pressure therapy. However, in the study conducted by Varan [54], pressure garments consist of nylon were treated with chitosan and the wireless pressure sensors were used to analyze the exerted pressure. The results showed that the exerted pressures of pressure garments were significantly increased after chitosan treatments. In the future study, we will investigate the materials of the pressure garments and the types of sensors in order to obtain better pressure therapeutic schedule.

In summary, we have established an effective animal model to examine the effect of pressure intervention on wound healing and scar formation. Our data strongly suggest that pressure improves the appearance and histology of scars. However, the results do not fully explain the precise mechanism: for example, we are yet to characterize the exact signal pathways involved in the process. Nevertheless, pressure intervention is an effective and noninvasive treatment method for scars. Hence, further cellular and molecular studies should be performed to delineate the mechanisms of this process and guide the development of a targeted molecular treatment for scars. In future, we intend to explore the molecular mechanisms of pressure in the fibroblasts extracted from normal human skin and hypertrophic scars.

Conflict of interest

The authors state no conflict of interest.

Acknowledgment

This work was supported by grants from the National Natural Science Fund of China (Nos. 11372208 and 31300771).

REFERENCES

[1] Bayat A, McGrouther DA, Ferguson MW. Skin scarring. BMJ 2003;326(7380):88–92.
[2] Alster TS, Tanzi EL. Hypertrophic scars and keloids. Am J Clin Dermatol 2003;4(4):235–43.
[3] van der Veer WM, Bloemen MC, Ulrich MM, Molema G, van Zuijlenet PP, Middelkoop E, et al. Potential cellular and molecular causes of hypertrophic scar formation. Burns 2009;35(1):15–29.
[4] Sidgwick GP, Bayat A. Extracellular matrix molecules implicated in hypertrophic and keloid scarring. J Eur Acad Dermatol Venereol 2012;26(2):141–52.
[5] Hsieh SC, Wu CC, Hsu SL, Yen JH. Molecular mechanisms of gallic acid-induced growth inhibition, apoptosis, and necrosis in hypertrophic scar fibroblasts. Life Sci 2017;179:130–8.
[6] Wang J, Dodd C, Shankowsky HA, Scott PG, Tredget EE. Deep dermal fibroblasts contribute to hypertrophic scarring. Lab Invest 2008;88(12):1278–90.
[7] Ud-Din S, Volk SW, Bayat A. Regenerative healing, scar-free healing and scar formation across the species: current concepts and future perspectives. Exp Dermatol 2014;23(9):615–9.
[8] Ud-Din S, Bayat A. New insights on keloids, hypertrophic scars, and striae. Dermatol Clin 2014;32(2):193–209.
[9] Anthonissen M, Daly D, Janssens T, van den Kerckhove E. The effects of conservative treatments on burn scars: a systematic review. Burns 2016;42(3):508–18.
[10] Gauglitz GG, Korting HC, Pavicic T, Ruzicka T, Jeschke MG. Hypertrophic scarring and keloids: pathomechanisms and current and emerging treatment strategies. Mol Med 2011;17(1–2):113–25.
[11] Edriss AS, Smrcka V. Therapy of keloid and hypertrophic scars: a review. Eur J Plast Surg 2011;34(6):425–36.
[12] Staley MJ, Richard RL. Use of pressure to treat hypertrophic burn scars. Adv Wound Care 1997;10(3):44–6.
[13] Macintyre L, Baird M. Pressure garments for use in the treatment of hypertrophic scars-a review of the problems associated with their use. Burns 2006;32(1):10–5.
[14] Candy LH, Cecilia LT, Ping ZY. Effect of different pressure magnitudes on hypertrophic scar in a Chinese population. Burns 2010;36(8):1234–41.
[15] Anzarut A, Olson J, Singh P, Rowe BH, Tredget EE. The effectiveness of pressure garment therapy for the prevention of abnormal scarring after burn injury: a meta-analysis. J Plast Reconstr Aesthet Surg 2009;62(1):77–84.
[16] Van den Kerckhove E, Stappaerts K, Fieuws S, Laperre J, Massage P, Flour M, et al. The assessment of erythema and thickness on burn related scars during pressure garment therapy as a preventive measure for hypertrophic scarring. Burns 2005;31(6):696–702.
[17] Gurtner GC, Dauskardt RH, Wong VW, Bhatt KA, Wu K, Vial IN, et al. Improving cutaneous scar formation by controlling the mechanical environment: large animal and phase I studies. Ann Surg 2011;254(2):217–25.
[18] Sharp PA, Pan B, Yakuboff KP, Rothchild D. Development of a best evidence statement for the use of pressure therapy for management of hypertrophic scarring. J Burn Care Res 2016;37(4):255–64.
[19] Ripper S, Renneberg B, Landmann C, Weigel G, Germann G. Adherence to pressure garment therapy in adult burn patients. Burns 2009;35(5):657–64.
[20] Puzey G. The use of pressure garments on hypertrophic scars. J Tissue Viability 2002;12(1):11–5.
[21] Rabello FB, Souza CD, Júnior JAF. Update on hypertrophic scar treatment. Clinics 2014;69(8):565–73.
[22] Macintyre L, Baird M, Weedall P. The study of pressure delivery for hypertrophic scar treatment. Int J Cloth Sci Tech 2004;16(1/2):173–83.
[23] Anand SC, Govarthanam KK, Gazioglu D. A study of the modelling and characterisation of compression garments for hypertrophic scarring after burns. Part 1: modelling of compression garments. J Text Inst 2013;104(7):661–7.
[24] Lai CH, Litsang CW. Validation of the Pliance X System in measuring interface pressure generated by pressure garment. Burns 2009;35(6):845–51.
[25] Morris DE, Wu L, Zhao LL, Bolton L, Roth SI, Ladin DA, et al. Acute and chronic animal models for excessive dermal scarring: quantitative studies. Plast Reconstr Surg 1997;100(3):674–81.
[26] Meyer W, Schwarz R, Neurand K. The skin of domestic mammals as a model for the human skin, with special reference to the domestic pig. Curr Probl Dermatol 1978;7(7):39–52.
[27] Montagna W, Yun JS. The skin of the domestic pig. J Invest Dermatol 1964;42(43):11–21.
[28] Gallant CL, Olson ME, Hart DA. Molecular, histologic, and gross phenotype of skin wound healing in red Duroc pigs reveals an abnormal healing phenotype of hypercontracted, hyperpigmented scarring. Wound Repair Regen 2004;12(3):305–19.
[29] Hu ZC, Tang B, Guo D, Zhang J, Liang YY, Ma D, et al. Expression of insulin-like growth factor-1 receptor in keloid and hypertrophic scar. Clin Exp Dermatol 2014;39(7):822–8.
[30] Ghahary A, Shen YJ, Wang R, Scott PG, Tredget EE. Expression and localization of insulin-like growth factor-1 in normal and post-burn hypertrophic scar tissue in human. Mol Cell Biochem 1998;183(1–2):1–9.
[31] Zha JP, Lackner MR. Targeting the insulin-like growth factor receptor-1R pathway for cancer therapy. Clin Cancer Res 2010;16(9):2512–7.
[32] Ishihara H, Yoshimoto H, Fujioka M, Murakami R, Hirano A, Fujii T, et al. Keloid fibroblasts resist ceramide-induced apoptosis by overexpression of insulin-like growth factor I receptor. J Invest Dermatol 2000;115(6):1065–71.
[33] Yoshimoto H, Ishihara H, Ohtsuru A, Akino K, Murakami R, Kuroda H, et al. Overexpression of insulin-like growth factor-1 (IGF-I) receptor and the invasiveness of cultured keloid fibroblasts. Am J Pathol 1999;154(3):883–9.
[34] Wu JH, Wang YH, Wang W, Shen W, Sang YZ, Liu L, et al. MiR-18b suppresses high-glucose-induced proliferation in HRECs by targeting IGF-1/IGF1R signaling pathways. Int J Biochem Cell Biol 2016;73:41–52.
[35] Girnita L, Worrall C, Takahashi SI, Seregard S, Girnita A. Something old, something new and something borrowed: emerging paradigm of insulin-like growth factor type 1 receptor (IGF-1R) signaling regulation. Cell Mol Life Sci 2014;71(13):2403–27.
[36] Zhu KQ, Engrav LH, Gibran NS, Cole JK, Matsumura H, Piepkorn M, et al. The female, red Duroc pig as an animal model of hypertrophic scarring and the potential role of the cones of skin. Burns 2003;29(7):649–64.
[37] Zhu KQ, Engrav LH, Tamura RN, Cole JA, Muangman P, Carrougher GJ, et al. Further similarities between cutaneous scarring in the female, red Duroc pig and human hypertrophic scarring. Burns 2004;30(6):518–30.
[38] Zhu KQ, Carrougher GJ, Gibran NS, Isik FF, Engrav LH. Review of the female Duroc/Yorkshire pig model of human fibroproliferative scarring. Wound Repair Regen 2007;15(Suppl. 1):S32–9.

[39] Li-Tsang CW, Feng BB, Huang L, Liu XS, Shu B, Chan YT, et al. A histological study on the effect of pressure therapy on the activities of myofibroblasts and keratinocytes in hypertrophic scar tissues after burn. Burns 2015;41(5):1008–16.

[40] Fraccalvieri M, Scalise A, Ruka E, Zingarelli E, Salomone M, Coda R, et al. Negative pressure wound therapy using gauze and foam: histological, immunohistochemical, and ultrasonography morphological analysis of granulation and scar tissues. Eur J Plast Surg 2014;37:411–6.

[41] Engrav LH, Heimbach DM, Rivara FP, Moore ML, Wang J, Carrougher GJ, et al. 12-year within-wound study of the effectiveness of custom pressure garment therapy. Burns 2010;36(7):975–83.

[42] Lian NQ, Li TP. Growth factor pathways in hypertrophic scars: molecular pathogenesis and therapeutic implications. Biomed Pharmacother 2016;84:42–50.

[43] Widgerow AD. Cellular/extracellular matrix cross-talk in scar evolution and control. Wound Repair Regen 2011;19(2):117–33.

[44] Ohtsuru A, Yoshimoto H, Ishihara H, Namba H, Yamashita S. Insulin-like growth factor-I (IGF-I)/IGF-I receptor axis and increased invasion activity of fibroblasts in keloid. Endocr J 2000;47(3):S41–4.

[45] Lesaint M, Balaji S, Bhattacharya SS, Moles CM, Kidd M, Dhamija Y, et al. Adenoviral-mediated gene transfer of insulin-like growth factor 1 enhances wound healing and induces angiogenesis. J Surg Res 2014;190(1):367–77.

[46] Emmerson E, Campbell L, Davies FC, Ross NL, Ashcroft GS, Krust A, et al. Insulin-like growth factor-1 promotes wound healing in estrogen-deprived mice: new insights into cutaneous IGF-1R/ERα cross talk. J Invest Dermatol 2012;132(12):2838–48.

[47] Sadagurski M, Yakar S, Weingarten G, Martin H, Rhodes CJ, Breitkreutz D, et al. Insulin-like growth factor 1 receptor signaling regulates skin development and inhibits skin keratinocyte differentiation. Mol Cell Biol 2006;26(7):2675–87.

[48] Gallant-behm CL, Olson ME, Hart DA. Cytokine and growth factor mRNA expression patterns associated with the hypercontracted, hyperpigmented healing phenotype of red duroc pigs: a model of abnormal human scar development? J Cutan Med Surg 2005;9(4):165–77.

[49] Hu XL, Wang HT, Liu JQ, Fang XB, Tao K, Wang YJ, et al. The role of ERK and JNK signaling in connective tissue growth factor induced extracellular matrix protein production and scar formation. Arch Dermatol Res 2013;305(5):433–45.

[50] Behm B, Babilas P, Landthaler M, Schreml S. Cytokines, chemokines and growth factors in wound healing. J Eur Acad Dermatol Venereol 2012;26(7):812–20.

[51] Huang D, Shen KH, Wang HG. Pressure therapy upregulates matrix metalloproteinase expression and downregulates collagen expression in hypertrophic scar tissue. Chin Med J 2013;126(17):3321–4.

[52] Varan NY. The effects of chitosan antimicrobial treatments on the physical and mechanical properties and wear performances of highly elastic fabrics used for burn scar management. J Text Inst 2018;109(1):39–45.

[53] Varan NY. Degree of chitosan deacetylation on antimicrobial properties of nylon 6,6 fabrics. AATCC J Res 2017;4(6):7–11.

[54] Varan NY. Wireless pressure sensors for pressure garments treated with chitosan. Int J Cloth Sci Technol 2017;29(5):732–42.